COMITATO NAZIONALE PER L'ENERGIA NUCLEARE
Laboratori Nazionali di Frascati

LNF -76/11(R)
20 Febbraio 1976

A.Renieri: TURBULENCE AND BUNCH LENGTHENING IN ELECTRON-POSITRON STORAGE RINGS. -

Servizio Documenlazione
dei laboralori Nazionali di Frascati del CNEN
Casella Postale 70 • Frascati (Rome)

Laboratori Nazi.onali di Frascati del CNEN
Servizio Documentazione

LNF-76jll(R)
20 Febbraio 1976

A. Renied: TURBULENCE AND BUNCH LENGTHENING IN ELEC-TRON-·POSITRON STORAGE RINGS.

1. - INTRODUCTION -

It has been observed[1÷3] that the bunch length in electron--positron storage rings is not in agreement with the theoretical predictions[4]. The theory takes into account only the effect of radiation noise and damping. It turns out (from the experiments) that the bunch lengt.h depends on the stored bunch current and on the beam energy. In addition a weak dependence on the accelerating r. f. voltage was observed at Adone. The experimental bunch length (in ACO and ADONE) is very well fitted by the following equation(2, 5, 24)

(1) $$\sigma_x^2 = \sigma_0^2 \; O\text{-}/\text{-} \; \frac{K\, I\, Va}{E_o^4\, \sigma_x}$$

with,

$$\alpha = \begin{cases} /.3 \text{ (ADONE)} \\ 0 \text{ (ACO)} \end{cases} \qquad K := \begin{cases} /2.10^{-2} \text{GeVxnsecxmA}^{-1}\text{x}\bar{\text{K}}\bar{\text{V}}^{-3} \text{ (ADONE)} \\ 2.10^{-3} \text{GeV}^4\text{xnsecxmA-1} \qquad \text{(ACO)} \end{cases}$$

σ_x = r. m. s. bunc'h length (experimental) (nsec)
σ_o = r. m. s. radiation bunch length (theoretical) (nsec)
I = bunch current (rnA)
Eo = working energy (GeV)
V = peak accelerating r. f. voltage (KV).

At ADONE(2) and SPEA.R(6) the lengthening effect is accompanied by an increase of the radial beam dimension. This effect may be explained by an increase of the energy spread in the bunch. One can not directly see a radial enlargement at ACO, because the transverse size measurements are performed in a point where the off-energy closed orbit function(4) is zero. However the increase of the energy spread occurs also in ACO and was observed by studying the excitation width of the synchrotron side-bands of the betatron frequency(7, 25). It is now possible to measure the energy spread of the two colliding (e+, 18-) beams, by using the recently discovered narrow resonances. At the particular energy of these resonances, there is agreement, at SPEAR(6), between transverse size measurements and experimental resonance width (one may neglect the natural width (~ 100 KeV) with respect to the machine energy spread (~ MeV)).

We want to recall now that the length and the energy spread, for a given bunch, depend on the bunch current only, meaning that a given bunch is not affected by the presence of the other ones. If therefore the lengthening effect is due to an interaction between bunch and storage ring elements, the merit Q-factor of these elements must be very low. We may then infer that the r. f. accelerating cavities cannot produce the effect. We have indeed observed that the behaviour of bunch lengthening at ADONE was not affected by the installation of two new r. f. cavities(2, 8) (the change was from two to four r. f. cavities).

2. - BUNCH LENGTHENING THEORIES -

We may divide the bunch lengthening theories into three classes, namely,

a) potential well modification(9, 10, 11)
b) longitudinal mode instabilities(12, 13)
c) Emission of coherent synchrotron radiation(14, 15).

The theories of the first group give a good fit of eq. (1), but do not explain the energy spread growth: any kind of potential well modification cannot change the natural radiation energy spread(16). Only if one adds accelerating r.f. noise(11), an energy spread increase can be obtained. The theories of the second group explain the anomalous energy spread, but the calculations made upto now only concern coasting beams, not bunched ones(26).

Thle theories of the last group predict bunch shortening. This effect has been observed only (at least up to now) in the storage ring for synchrotron radiation TANTALUS 1(17).

In this paper we extend the theories of the second group (longitUdinal mode instabilities) to bunched beams. We show that, above a given threshold, the longitudinal equilibrium distribution function satisfying the Fokker··Planck equation(18) is unstable. This threshold depends on the bunch current, bea.m ene'rgy, radiation energy spread an.d radiation damping.

At the. threshold we have the "hydrodyn.amic transition",

$$\boxed{\text{Laminar motion}} \Longrightarrow \overline{\text{strongly turbulent collective motion}}$$

(following Sessler's notations(13)).

Below the threshold we have merely a bunch lengthening due to the potential well :rnodification. Above the threshold we have also an increase of the energy spread within the: bunch.

3. - FOKKER-PLANCK EQUATION FOR SYNCHROTRON MOTION. -

The recurrence equations (turn by turn) of the synchrotron motion are(19, 20), (wle have neglected radiation noise and damping) -

$$(2) \qquad \begin{cases} \tau_h(n) - \tau_h(n-1) = \Lambda\, \varepsilon_h(n) \\ \varepsilon_h(n+1) - \varepsilon_h(n) = eV\sin(\omega_o B\, \tau_h(n) + \phi_o) + W, \end{cases}$$

Where we have defined,

$\tau_K(n)$, $\varepsilon_K(n)$ = time and energy displacement of the Kth particle, from the synchronous one at the nth turn.

$\omega_o :: 2\pi/T$ = machine revolution frequency

V, 13, ϕ_o = peak voltage, harmonic number and phase of the accelerating r. f. system.

e = lelectron charge

W :: mean energy lost per turn by synchrotron radiation

$\Lambda = (2\pi\alpha)/(\omega_o E_o)$, α = momentum compaction

E_o :: working energy.

The r.f. synchronous phase ϕ_o is given by eq. (2), with the conditions,

$$\tau_h(n) = 0, \qquad \varepsilon_h(n) = 0,$$

that is,

$$eV\sin\phi_o = -W \tag{3}$$

We assume that in the machine there is an element (like a spurious cavity) which has a longitudinal coupling impedance to the beam. In this paper we consider a very simple case, but the method may be extended to whatever (more realistic:) impedance. We actually assume to have a simple RC element. The current I(t) of a bunch of N particles of charge e (seen by the element we are considering) is given by,

$$I(t) = e \sum_{K=1}^{N} \delta\ (t - \tau Fe) \tag{4}$$

where δ (t) is the Dirac δ-function and τk is the time displacement of the Kth particle from the synchronous one (we assume that the time of passage of the synchronous particles is t = 0). The longitudinal voltageacross the RC element at time t, produced by current l(t) (see eq. (4)), is given by,

$$Vet) = e\ 2_0\ r \sum_{K=1}^{N} e\text{-}\ r(t\cdot.\ ^{\tau}K)\theta\ (t-\tau_K) \tag{5}$$

where $1/r$ is the signal decay time in the RC element and $\theta(x)$ is the step function, defined by,

$$\theta(x) = \begin{cases} 1 & \text{if } x > 0 \\ 0 & \text{if } x < 0 \end{cases} \tag{6}$$

In eq. (5) we consider only one passage. We actually assume that the signal decay time is shorter than the revolution period T, that i.s;

$$T r' > 1. \tag{7}$$

This is in agreement with the observationthat the lengthening effect is a single bunch phenomenon.

The voltage seen by the h^{th} particle (with time passage τ_h)

is given by,

$$V(\tau_h) = eZ_o \Gamma \sum_{K=1}^{N} e^{-\Gamma(\tau_h - \tau_K)} \theta(\tau_h - \tau_K) \tag{8}$$

We point out that particle h sees particle k only if, (causality condition)

$$\tau_h > \tau_k \quad (\Rightarrow \theta(\tau_h - \tau_k) = 1) \tag{9}$$

If we add eq. (8) to the r.h.s. of the second equation of system (2), and if we recall eq" (3) we obtain,

$$\begin{cases} \tau h(n) - \tau_h(n-1) = \lambda \quad \varepsilon h(n) \\ \varepsilon h(n+1) - \varepsilon_h(n) = eV(\sin(\omega_o B \tau_h(n) + \phi_o) - \sin\phi_o) + \\ \qquad + e^2 Z_0 \Gamma \sum_{K=1}^{N} e^{-\Gamma(\tau_h(n) - \tau_k(n))} \theta(\tau_h(n) - \tau_k(n)). \end{cases} \tag{10}$$

The synchrotron oscillation is a very slow motion with respect to the revolution time. Therlefore we may substitute the difference equations with the di.fferential ones. Namely

$$\tau_h(n) - \tau_h(n-1) \quad \text{becomes} \quad T \, d\tau_h/dt$$

and

$$\varepsilon_h(n+1) - \varepsilon_h(n) \quad \text{becomes} \quad T \, d\varepsilon_h/dt$$

Finally, if we lineari.ze the r"f. voltage around the synchronous phase (small oscillations), eq. (10) becomes.

$$\begin{cases} \dfrac{d\tau_h}{dt} = -\dfrac{\omega_o \lambda}{2\pi} \\ \dfrac{d\varepsilon_h}{dt} = -\dfrac{\omega_o^2 eVB\cos\phi_o}{2\pi} \qquad \dfrac{e^2 Z_o \Gamma \omega_o}{2\pi} \sum_{K=1} e^{-\Gamma(\tau_h - \tau_k)} \theta(\tau_h - \tau_k). \end{cases} \tag{11}$$

Let us define now the new variables,

$$x_h = \omega_o \Omega_0 \tau_h$$

(12) $$y_h = a\,(\varepsilon_h / E_0)$$

$$\theta = \Omega_o \omega_0 t$$

and

(13) $$\Omega_o^2 = \frac{eV_a B\cos\phi_o}{2\pi E_o} \qquad \eta = \frac{e^2 Z_o \Gamma N\alpha}{2\pi E_o \Omega_0} \qquad \mu = \frac{I'}{\omega_o \Omega_0}$$

($\omega_o \Omega_0$ = synchrotron frequency).

We obtain,

(14) $$\begin{cases} \dfrac{dx_h}{d\theta} = y_h \\ = -x_h + \eta\left(\dfrac{1}{N}\displaystyle\sum_{K=1}^{N} e^{-\mu(x_h - x_k)}\,\theta(x_h - x_k)\right). \end{cases}$$

The number of particles in the bunch is usually very high ($N \sim 10^{10}$), so that we may consider it as continuous. We can define the synchrotron distribution function,

$$f_o(x, y \mid \theta)$$

This function must satisfy the normalization c oudition,

(15) $$\int_{-\infty}^{+\infty} dx \int_{-\infty}^{+\infty} dy\, f_o(x, y \mid \theta) = 1$$

Eq. (15) becomes,

(16) $$\begin{cases} \dfrac{dx}{d\theta} = y \\ \dfrac{dy}{d\theta} = -x + \eta \displaystyle\int_{-\infty}^{+\infty} dx_o \int_{-\infty}^{+\infty} dy_o\, \theta(x - x_o) f(x_o, y_o \mid \theta) \end{cases}$$

Where we define,

$$\varrho_0(x) = e^{-\mu x}\,\theta(x). \tag{17}$$

From eq. (16) we may derive the Fokker-Planck (F.P.) equation[18] for the distribution function $f_0(x, y \mid \theta)$,

$$\frac{\partial f_0}{\partial \theta} + y\frac{\partial f_0}{\partial x} - \left\{x + \frac{2y}{\tau} - \eta\int_{-\infty}^{+\infty} dy_0 \int_{-\infty}^{+\infty} dx_0\, \varrho_0(x-x_0) f_0(x_0, y_0 \mid \theta)\right\}\times$$

$$\times\frac{\partial f}{\partial y} - \frac{2}{\tau} f_0 - \frac{2\sigma^2}{\tau}\frac{\partial^2 f_0}{\partial Y^2} = 0, \tag{18}$$

Where we have.

$\tau/(\omega_0\Omega_0)$ = longitudinal radia.tion darnping time,

σ_p/α = r.m.s. relative radiation energy width.

For $\eta = 0$, the time independent solution of eq. (18) is,

$$f_0(x,y) = \frac{1}{2\pi\sigma_p^2}\, e^{\frac{x^2+y^2}{2\sigma_p^2}} \tag{19}$$

We shall see later (sect. 6) that this solution is not only stable, but it is the limit distribution function for $t \to \infty$.

Let us define the new· "norma111 variables.

$$\xi = \frac{x}{\sigma_p}, \qquad \zeta = \frac{y}{\sigma_p} \tag{20}$$

if we put,

$$\begin{cases} f_0(x, y \mid \theta)dxdy = f(\xi, \zeta \mid \theta)d\xi\, d\zeta \\ \varrho_0(x) = \varrho(\xi) = e^{-\mu\sigma_p \xi}\,\theta(\xi) \\ \varepsilon = \dfrac{\eta}{\sigma_p} \end{cases} \tag{21}$$

eq. (18) becomes

$$\frac{\partial f}{\partial \theta} + \zeta \frac{\partial f}{\partial \xi} - (\xi + \frac{2}{\tau}\ \zeta - \varepsilon \int_{+\infty}^{+\infty} d\zeta_o \int_{-\infty}^{+\infty} d\xi_o\, \varrho(\xi - \xi_o) f(\xi_o, \zeta_o | \theta)) \times$$

(22)

$$\times \frac{\partial f}{\partial \zeta} - \frac{2}{\tau} (f + \frac{\partial^2 f}{\partial \zeta^2}) = 0$$

4. - TIME INDEPENDENT SOLUTION OF THE F.P. EQUATION. -

The time-independent distribution that satisfies the F.P. equa·-tion may be written in the form

(23)
$$f(\xi, \zeta) = \frac{1}{\sqrt{2\pi}} e^{-\frac{\zeta^2}{2}}\ g(\xi) \left(\int_{-\infty}^{+\infty} g(\xi) d\xi = 1 \right),$$

where $g(\xi)$ satisfies the equation,

(24)
$$\frac{dg(\xi)}{d\xi} + \xi\, g(\xi) = \varepsilon g(\xi) \int_{-\infty}^{+\infty} \varrho(\xi - \xi_o) g(\xi_o) d\xi_o .$$

Eq. (24) may be easily integrated by using numerical met.hods. In Fig. 1, as an example, we have the function $g(\xi)$ for the following parameter values,

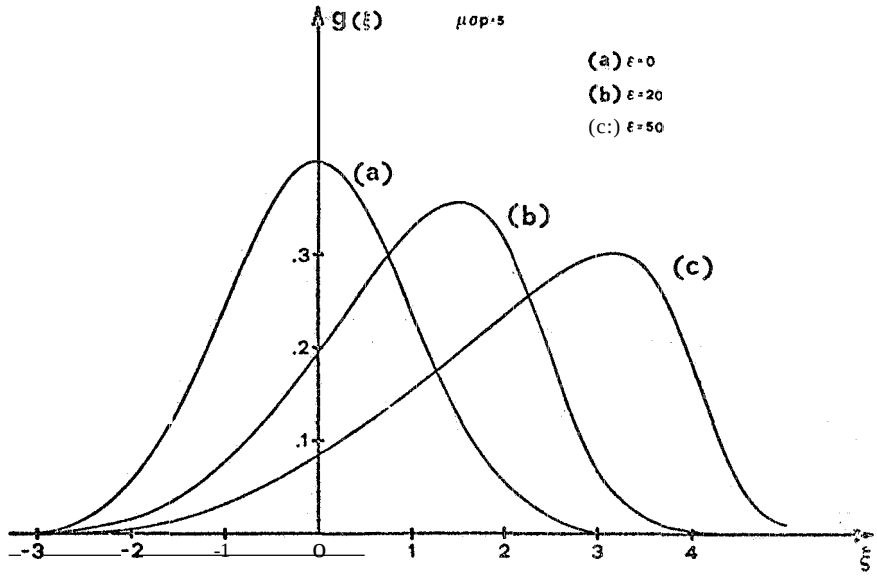

FIG. 1

$$\mu\sigma_p = 5; \qquad \varepsilon = 0,\ 20,\ 50.$$

For $\varepsilon = 0$ we have the unperturbated distribution (see also eq. (19)),

$$g_{\varepsilon=0}(\xi) = \frac{1}{\sqrt{2\pi}}\, e^{-\xi^2/2}$$

From eq. (23) we see that the time-independent longitudinal distribution function has the same ζ-dependence as the zero current ($\varepsilon = 0$) solution (that is the same energy spread dependence). At the same time the ξ distribution is also modified (potential well modification). This is just the behaviour predicted by Hereward(16).

We may test the numerical solution of eq. (24) by using a computer simulation of the synchrotron motion.

Let us consider again the difference equations (10). If we take into account the noise and the damping (τ) due to the radiation processes, eq. (10) becomes(20), (using the (ξ, ζ) variables),

$$\xi_h(n) - \xi_h(n-1) = 2\pi\Omega_0\, \zeta_h(n)$$

(25)

$$\zeta_h(n) - \zeta_h(n-1) = -\frac{2}{\tau}\,\zeta_h(n-1) + \varepsilon\left(\frac{1}{N}\sum_{K=1}^{N} e^{-\mu\sigma_p(\xi_h(n)-\xi_k(n))}\,\theta(\xi_h(n)-\xi_k(n))\right) + A\,Z_n$$

The damping is given by the term,

$$2\pi\Omega_0\left(-\frac{2}{\tau}\,\zeta_h(n)\right)$$

an the noise due to the quantum fluctuations

$$A\,Z_n$$

where we have

(26)

$$A = \sqrt{\frac{4}{\tau}}\,(2\pi\Omega_0)$$

and r_n is a random function that satisfies the equations, ($<\ >$ means mean value)

(27) $$< r_n^2 > = 1, \quad < r'_n > = 10$$

In Fig. 2a we have plotted with solid line the $g(\xi)$ distribution derived from the F. P. equation (24), for $\varepsilon = 30$, $\mu\sigma_p = 5$. In this case we have simulated the longitudinal bunch motion with eq. (25), for a bunch consisU,ng of,

N = .number of particle = 10^3 (the limit on N is given by the computer time available)

in the following conditions,

$$\tau : 10, \qquad \Omega_o = 10^{-2}$$

This ,means that a complete synchrotron period is covered in a number of machine turns given by,

(28) $$N_S = \frac{1}{\Omega_o} = 100$$

and the number of turns per damping time is,

(29) $$N_D = \frac{\tau}{\Omega_o 2\pi} = \frac{10^3}{2\pi} \cong 160$$

The discontinous line (-0-0-) shows (in fig. 2a) the starting distribution $go(\xi)$. We have chosen $go(\xi)$ just equal to the unperturbed one ($\varepsilon = 0$), that is,

$$g_o(\xi) = \frac{1}{\sqrt{2\pi}} e^{-\xi^2/2}$$

Finally (crosses x) we have plotted the distribution given by eq.(25) after 4 x 10^3 turns, that is after 40 synchrotron periods (see eq. (28)) and after 25 time radiation damping constants (see eq. (29))" We have a very good agreement between the simulation and the theoretical prediction. The ζ -distribution after 4 x 10^3 turns is plotted in fig. 2b.-

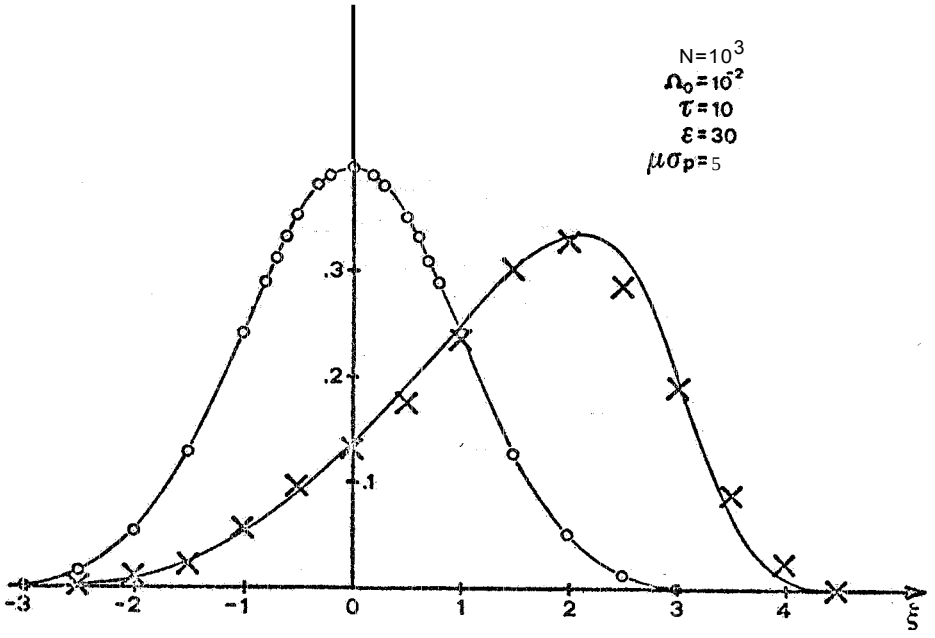
N=10^3
Ω0=10^-2
τ=10
ε=30
μσp=5
.3
.2
.1
-3
-2
-1
0
1
2
3
4
ξ

(a)

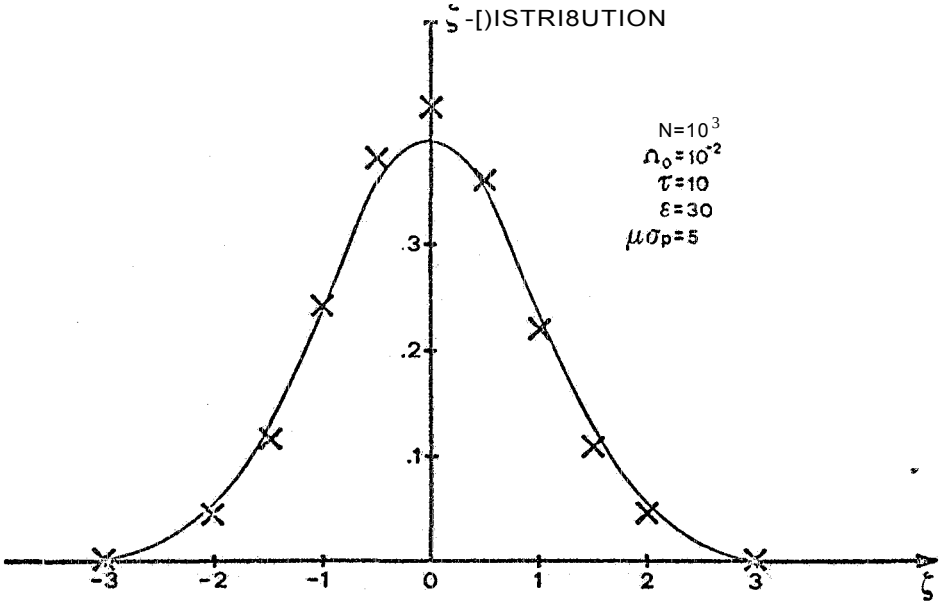
ζ-DISTRIBUTION
N=10^3
Ω0=10^-2
τ=10
ε=30
μσp=5
.3
.2
.1
-3
-2
-1
0
1
2
3
ζ

(b)

FIG. 2

We have again a complete agreement between the F. P. distribution (solid line) and the simulation (crosses).

This behaviour is not quite general. It happens that, for fixed τ and $\mu\sigma_p$' we have a threshold in ε · For $\varepsilon < \varepsilon_{th}$ there is agreement between simulation and time-independent F. P. equation. For $\varepsilon > \varepsilon_{th}$ there is no agreement. In particular the width of both the ξ and ζ simulated distributions are bigger than the calculated ones. We may use, as a parameter for the simulated distribution, the quantity,

$$\Delta_n = \frac{\sigma_\zeta^2(n) - 1}{2} \tag{30}$$

where $\sigma_\zeta(n)$ isthe.r.m. s. width in ζ at the nth turn, that is,

$$\sigma_\zeta^2(n) = \frac{1}{N}\sum_{K=1}^{N}\zeta_K^2(n) - \left(\frac{1}{N}\sum_{K=1}^{N}\zeta_K(n)\right)^2 \tag{31}$$

We have plotted Δ_n versus n in Fig. 3 in the conditions,

(a) $\varepsilon = 12.5$
(b) $\varepsilon = 37.5$
$\mu\sigma_p = 5, \quad \tau = 200, \quad \Omega_o = 10^{-2}$

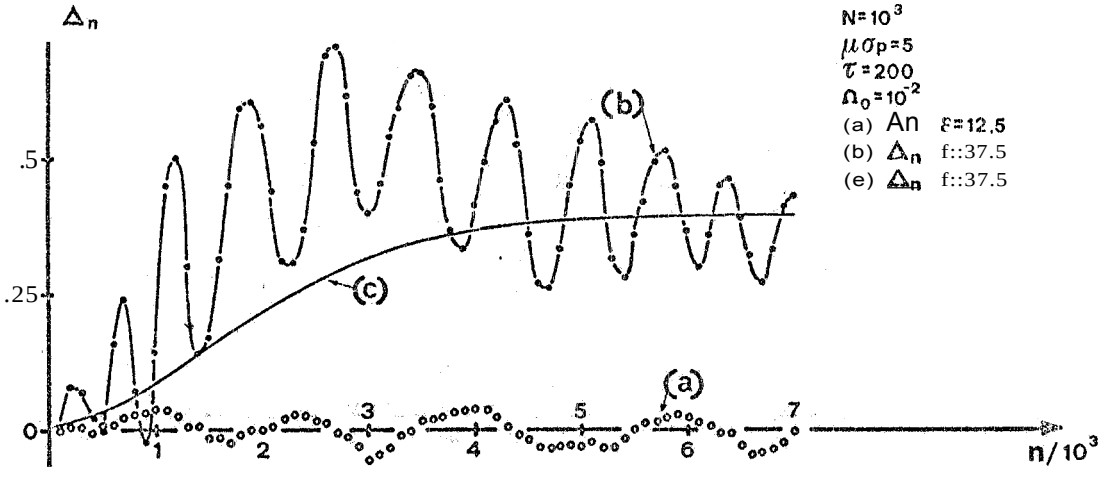

FIG. 3

and with the starting distribution defined by the F. P. equation. More exactly we may say that the curves (a) and (b) represent the sampling

of Δ_n at the synchrotron frequency. What is actually plotted is the value of Δ_n every 10^2 machine turns (remember eq. (28)).

Curve (a) oscillates around zero (agreement between F, P. equation and simulation). The oscillations may depend on the finite number ($N = 10^3$) of particles in the bunch.

Curve (b) shows that the simulation gives a broader ζ-distribution, which therefore does not agree with the F. P. time-independent equation. In a order to avoid unwanted osdllations, we plot, in fig. 3, the quantity, (solid line (c)),

$$\bar{\Delta}_n = \frac{1}{n} \sum_{m=1}^{n} \Delta_m \tag{32}$$

under condition (b) ($\varepsilon = 37.5$). This function ($\bar{\Delta}_n$) gives a better idea of the limit distribution for $n \to \infty$ (if it there is!).

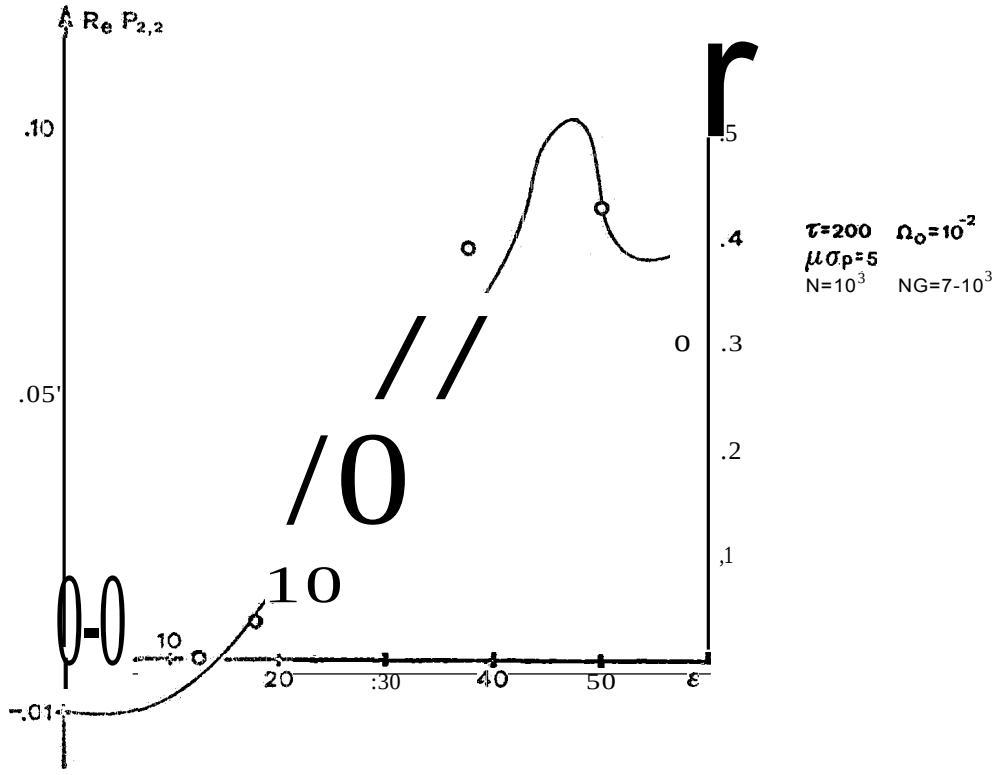

FIG. 4

In fig. 4 it is plotted (with dots) the quantity $\bar{\Delta}$ versus ε in the following conditions, $n = 7 \times 10^3$ (this limit is given by the available computer time),

$$\tau = .200, \qquad \mu\sigma :: 5, \qquad \Omega_o = 10^{-2}$$

The solid line will be explained later. We may see that, for $\varepsilon > 12.5 \div 18$, the width of the simulated ζ distribution blows up (up to about 50%). We may expect that this behaviour is due to the instability of the distribution (23). To test this hypothesis we will study, in the following sections, the behaviour of the F. P. equation around the time-independent solution (23).

5. - HERMITE DEVELOPMENT OF THE F. P. EQUATION.-

Let us develop the distribution $f(\xi, \zeta/\theta)$ into Hermite orthogonal polynomials(21). We have,

$$(33) \quad f(\xi, \zeta/\theta) = \frac{1}{2\pi} \sum_{n=0}^{\infty} \sum_{m=0}^{\infty} f_{n,m}(\theta) H_{en}(\xi - \bar{\xi}) H_{em}(\zeta) e^{-\frac{(\xi-\bar{\xi})^2+\zeta^2}{2}}.$$

where $\bar{\xi}$ is the center of mass of the time-independent distribution, (see eqs. (23) and (24)),

$$(34) \quad \int_{-\infty}^{+\infty} \xi\, g(\xi)\, d\xi$$

we develop around $\bar{\xi}$ in order to have a faster convergence in the series(33).

From the orthogonality relations of the Hermite polynomials, we obtain,

$$(35) \quad f_{n,m}(\theta) = \frac{1}{n!\,m!} \int_{-\infty}^{+\infty} d\xi \int_{-\infty}^{+\infty} d\zeta\, H_{en}(\xi - \bar{\xi}) H_{em}(\zeta) f(\xi, \bar{\zeta}/\theta).$$

The normalization condition becomes,

$$(36) \quad \int_{-\infty}^{+\infty} d\xi \int_{-\infty}^{+\infty} d\zeta\, f(\xi, \zeta \mid \theta) = f_{o,o}(\theta) = 1$$

If we insert eq. (33) into eq. (22) and if we use the following condition,

$$(37) \quad f_{h,k}(\theta) \neq 0 \qquad \text{only if} \quad h \geq 0 \qquad \text{and} \quad K \geq 0$$

We obtain, (using the notation $f'_{n,m} = df_{n,m}/d\theta$)

$$f'_{n,m} - (m+1)f_{n-1,m+1} + (n+1)f_{n+1,m-1} + \frac{2m}{\tau} f_{n,m} =$$

$$(38) \qquad = \varepsilon \sum_{s=0}^{\infty} \sum_{h=0}^{\infty} A^{n}_{s,h} f_{s,s} f_{h,m-1} - \bar{\xi} f_{n,m-1}$$

$$(n, m = 0, 1, 2, \ldots,.)$$

where we define

$$(39) \qquad A^{n}_{s,h} = \frac{1}{2\pi n!} \int_{-\infty}^{+\infty} d\xi \int_{-\infty}^{+\infty} d\xi_0 \, e^{-\frac{\xi^2 + \xi_0^2}{2}} \varrho(\xi - \xi_0) H_{es}(\xi_0) H_{eh}(\xi) H_{en}(\xi).$$

Firstly we point out that the condition (36) is always satisfied. Eq. (38) becomes indeed (for m = n = 0),

$$(40) \qquad \frac{df_{0,0}}{d\theta} = 0 \Rightarrow f_{0,0}(\theta) = \text{const.} = 1.$$

In order to understand (see next section) the physical meaning of the Hermite coefficients $f_{n,m}$ it is useful to change their labels. Namely we put,

$$(41) \qquad h_{l,r} = f_{r,l-r} \qquad (0 \leq l < \infty; \quad 0 \leq r \leq l)$$

that is,

$$f_{n,m} = h_{n+m,n} \qquad (0 \leq n, m < \infty)$$

Eq. (38) becomes

$$h'_{l,n} - (l-n+1)h_{l,n-1} + (n+1)h_{l,n+1} + \frac{2(l-n)}{\tau} h_{l,n} =$$

$$(42) \qquad = \varepsilon \sum_{s=0}^{\infty} \sum_{h=0}^{\infty} A^{n}_{s,h} h_{s,s} h_{h+l-n-1;h} - \bar{\xi} h_{l-1,n}.$$

Condition (37) becomes,

$$(43) \qquad h_{l,n} \not\equiv 0 \quad \text{only if} \quad l \geq 0 \quad \text{and} \quad 0 \leq n \leq l.$$

6. - PHYSICAL MEANING OF THE HERMITE COEFFICIENTS -

For zero current we have $\varepsilon = 0$ and $\bar{\xi} = 0$. Then eq.(43) becomes, $(1 = 0,1,2, \ldots ; 0 \leq n \leq 1)$

$$(44) \quad h'_{1,n} - (1-n+1)h_{1\,n-1} + (n+1)h_{1\,n+1} + 2\frac{1-n}{\tau} h_{1,n} = 0$$

In this condition the set of infinite equations: (42) is broken into finite sets of $(1 + 1)$ equations, which can be easily integrated. We have indeed;

$\underline{1 = 0;\ n = 0}$, normalization condition

$$h'_{0,0} = 0, \quad h_{00} = 1$$

The eigenfrequency p of this mode is given obviously by,

$$p = 0$$

$\underline{1=1;n=0,1}$ dipole mode

$$\begin{cases} h'_{1,0} + h_{1,1} + \frac{2}{\tau} h_{1,0} = 0 \\ h'_{1,1} - h_{1,0} = 0 \end{cases}$$

The eigenfrequencies p are the roots of the secular equation, (as usually $i = \sqrt{-1}$)

$$\begin{vmatrix} p + \frac{2}{\tau}, & 1 \\ -1, & p \end{vmatrix} = 0 \quad \Rightarrow p^2 + \frac{2}{\tau} p + 1 = 0 \Rightarrow p = -\frac{1}{\tau} + i\sqrt{1 - \frac{1}{\tau^2}}$$

$\underline{1=2;n=0,1,2:}$, quadrupole mode

$$\begin{cases} h'_{2,0} + h_{2,1} + \frac{4}{\tau} h_{2,0} = 0 \\ h'_{2,1} - 2h_{2,0} + 2h_{2,2} + \frac{3}{\tau} h_{2,1} = 0 \\ h'_{2,2} - h_{2,1} = 0 \end{cases}$$

We have,

$$\begin{vmatrix} p+\frac{4}{\tau}, & 1 & 0 \\ -2 & , p+\frac{2}{\tau} & 2 \\ 0 & -1 & p \end{vmatrix} = 0 \Rightarrow (p+\frac{2}{\tau})(p^2+\frac{4}{\tau}p+4) = 0$$

so that we obtain,

$$p = -\frac{2}{\tau}; \qquad p := 2\left(-\frac{1}{\tau} \pm i\sqrt{1-\frac{1}{\tau^2}}\right)$$

$l = 3$; $n = 0, 1, 2, 3$ sextupole mode

the eigenfrequencies are,

$$p = -\frac{3}{\tau} \pm i\sqrt{1-\frac{1}{\tau^2}} \qquad p = 3\left(-\frac{1}{\tau} \pm i\sqrt{1-\frac{1}{\tau^2}}\right)$$

and so on.

In general we have,

a) even modes ($l = 2m$)

$$p^{\pm}_{2m,2n} = -\frac{2m}{\tau} \pm 2ni\sqrt{1-\frac{1}{\tau^2}} \qquad (0 \le n \le m) \tag{45}$$

b) odd modes ($l = 2m + 1$)

$$p^{\pm}_{2m+1,\,2n+1} = -\frac{2m+1}{\tau} \pm (2n+1)i\sqrt{1-\frac{1}{\tau^2}} \qquad (0 \le n \le m). \tag{46}$$

We may see that, except for the mode ($l = 0$, $n = 0$), the real part of the eigenfrequencies (45), (46) is always negative. That is all modes with $l \neq 0$ disappear for $t \to \infty$. There remains only the ($l = 0$, $n = 0$) mode, whieh corresponds to the time-independent (gaussian) distribution (19).

We may represent the Hermite coefficients by using the, following array, (see Tab. I).

Dilfferent modes are independent. Only the terms which belong to the same line are interacting.

The situation changes when $\varepsilon \neq 0$ (and $\tilde{\xi} \neq 0$). In this case all

modes are coupled, via the r.h. s. of eq. (42).

TABLE I

$h_{o,o}$	normalization
$h_{1,o}$, $h_{1,1}$	dipole
$h_{2,0}$, $h_{2,1}$, $h_{2,2}$	quadrupole
$h_{3,0}$, $h_{3,1}$, $h_{3,2}$, $h_{3,3}$	sextupole
$h_{1,0}$, $h_{1,1}$, $h_{1,2}$, $h_{1,3}$, ... $h_{I,1}$	l-pole

7. - LINEAR DEVELOPMENT AROUND THE TIME-INDEPENDENT DISTRIBUTION $\bar{f}(\xi,\zeta)$. -

Let us develop the eq. (48)around the time-independent distribution (23) $(\bar{f}(\xi,\zeta))$.

It is possible to derive $\bar{f}(\xi,\zeta)$ directly from eq. (42), by putting,

$$h'_{l,n} = 0 \qquad (l=0,1,2,\ldots;\ n = 0,1,2,\ldots,l) \tag{47}$$

We obtain,

$$h_{o,o} = 1,\ \bar{h}_{l,n} = 0 \text{ if } l \neq n$$

$$l \cdot \bar{h}_{l,l} = \varepsilon \sum_{s=0}^{\infty} \sum_{h=0}^{\infty} A^{l-1}_{s,h} \bar{h}_{s,s} \bar{h}_{h,h} - \xi \bar{h}_{l-1,l-1} \tag{48}$$

$$(l=1,2,\ldots.)$$

Of course we have,

$$\bar{f}(\xi,\zeta) = \frac{1}{\sqrt{2\pi}}\, l^{-\zeta^2/2} \left(\frac{1}{\sqrt{2\pi}} \sum_{s=0}^{\infty} \bar{h}_{s,s} H_{es}(\xi-\bar{\xi})\right) l^{\frac{(\xi-\bar{\xi})^2}{2}} \tag{49}$$

That is,

$$g(\xi) = \frac{1}{\sqrt{2\pi}} \sum_{s=0} h_{s} H_{s}(\xi - \bar{\xi}) 1^{-(\xi - \bar{\xi})^2 / 2} \tag{50}$$

Then, in addition to eq. (48), we have the equation, (see eqs. (34) and (50)),

$$\bar{\xi} = \int_{-\infty}^{+\infty} \xi g(\xi) d\xi = \bar{h}_{0,0} \bar{\xi} + \bar{h}_{1,1} = \bar{h}_{1,1} + \bar{\xi} \Rightarrow \bar{h}_{1,1} = 0 \tag{51}$$

Let us define the variables,

$$z_{1,n} = h_{1,n} - h_{1,n} \qquad (z_{0,0} = 0). \tag{52}$$

To the first order in $z_{1,n}$ eq. (42) becomes,

$$\begin{cases} z'_{1,0} + z_{1,1} + \frac{21}{\tau} z_{1,0} = \varepsilon \sum_{h=0}^{\infty} S_h^0 z_{h+1-1,h} - \bar{\xi} z_{1-1,0} \\ z'_{1,n} - (1-n+1) z_{I,n\cdot\cdot 1} - (n+1) z_{1,n+1} + 2 \frac{I-n}{\tau} z_{1,n} = \varepsilon \sum_{h=0}^{\infty} S_h^n z_{h+I-n-1,h} - \bar{\xi} z_{1-1,n} \\ z'_{1,1-1} - 2 z_{1,1-2} + 1 z_{1,1} + \frac{2}{\tau} z_{1,1-1} = \varepsilon \sum_{h=1}^{\infty} P_h^{1-1} z_{h,h} - \bar{\xi} z_{1-1,1-1} \\ z'_{1,1} - z_{1,1-1} = 0 \\ (1 = 1,2, \ldots\ldots) \end{cases} \tag{53}$$

where we define,

$$P_h^{11} = \sum_{s=o}^{\infty} (A_{s,h}^{n} + A_{h,s}^{n}) h_{s,s}$$

$$S_h^n = \sum_{s=o}^{\infty} A_{s.,h}^{n} \bar{h}_{s,s} \tag{54}$$

In order to evaluate the eigenfrequencies of the system (53), we must consider a finite number M of oscillation modes. The order of such a system is given by.,

$$N_M = \frac{(M+1)}{2}\frac{(M+2)}{} - 1 \qquad (55)$$

N_M is in fact the number of the elements of the following array,

$$2_{1,0}\ ^2\ 1,1$$

$$Z2,0\ \ Z2,1\ \ 2_{2,2}$$

$$Z_{M,0}\ Z_{M,1}\ Z_{M,2}\ \text{-----}\ \ ZMM$$

The order (NM) increases rapidly 'with M. For example, for N = 9 wehave N_M = 44 and for N = 10, N_M = 6,5. This fact gives a strong limitation to the maximum number of modes that we ma.y consider. We have checked that the choice,

$$M = 10\ (N_M = 65)$$

is sufficient for a good evaluation of the lower mode eigenfrequencies (l = 1, 2, 3, 4), in the range of ε and $\mu\sigma P$ that we have investigated (the change from M= 9 to M= 10 does not affect the results by more than 10%).

8. - EIGENFREIQlJENCIES AND STABILITY CONDITION -

In sec. 6 we have developed the bunch motion (for ε = 0) into its normal modes. The frequencies are given by eqs. (45) and (46). We shall label with the symbol,

$$(l,\ n)$$

the mode corresponding to the eigenfrequency for zero current,

$$p_{l,}^{\pm}\ n = -\frac{1}{\tau} \pm in\sqrt{1 - \frac{1}{\tau}^2}$$

with

$$l \geq 1, \qquad 0 \leq n \leq l, \qquad n \text{ has the same parity as } l.$$

When we have $\varepsilon \neq 0$, all modes are coupled together and their frequencies change" In particular, the real part may become positive" In this condition the time-indepEmdent solution becomes unstable" We may expect (and we shall see later that this actually happens) that the growth of bunch dimension a.nd internal energy spread, occurs just when the quadrupole modes become unstable (modes (2,0) and (2, 2)). These modes are indeed related to the third line in tab. 1 (quadrupole line), that is to,

$$h_{2,0}, \qquad h_{2,1},$$

From eqs. (35) and (41) we have[21],

$$h_{2,0} = f_{2,0} = \frac{1}{2} \int_{-\infty}^{+\infty} d\xi \int_{-\infty}^{+\infty} d\zeta H_{e2}(\zeta) f(\xi, \zeta \mid \theta) =$$

(56)

$$= \frac{1}{2} \int_{-\infty}^{+\infty} d\xi \int_{-\infty}^{+\infty} d\zeta (\zeta^2 - 1)\, f(\xi, \zeta \mid \theta) = \frac{1}{2} (\langle \zeta^2 \rangle - 1),$$

in the same way we obtain,

$$h_{2,1} = f_{1,1} = \langle \xi \zeta \rangle - \bar{\xi} \langle \zeta \rangle$$

(57)

$$h_{2,2} = \frac{1}{2} \left(\langle \xi^2 \rangle - 2 \langle \xi \rangle \bar{\xi} + \bar{\xi}^2 - 1 \right)$$

We remark that in general

$$\bar{\xi} \neq \langle \xi \rangle$$

where $\bar{\xi}$ is the center of mass of the time-independent distribution $g(\xi)$ (see eq. (34)), while $\langle \xi \rangle$ is the center of mass of the more genera.l time-dependent distribution $f(\xi, \zeta \mid \theta)$, that is,

$$\langle \xi \rangle = \int_{-\infty}^{+\infty} d\zeta \int_{-\infty}^{+\infty} \xi\, d\xi f(\xi, \zeta \mid \theta).$$

We may expect that, if mode (2, 0) (or (2,2)) becomes unstable, the term (for example)

(58) $$h_{2,0} = \frac{1}{2}(<\zeta^2> - 1)$$

blows up.

In fig. 4 we ,have plotted (solid line), together with $\bar{\Delta}$ (see eq. (32»), the real part of mode (2, 2) $OR_{eP2,2}$) for $\tau = 200$ and $\mu\sigma_p = 5$. There is a good agreement between the threshold given by the equation,

$$\mathbb{R}_e p_{2,2} = 0$$

and the behaviour of $\bar{\Delta}$ We want to recall that Δ is closely related to the Hermite coefficient $h_2, 0$ (see eqs. (31) and (5,6»).

Let us define,

$$\delta = \frac{\sigma_\xi^2 - 1}{2}$$

where σ_ξ is the r. m. s. width of the time-independent distribution function g(ξ),

$$\sigma_\xi^2 = \int_{-\infty}^{+\infty} \xi^2 d\xi\, g(\xi) - \bar{\xi}^2$$

In fig. 5 it is plotted δ versus ε for $\mu\sigma_p = 0,2,5$.

We prefer to use δ instead of ε , because it gives us more directly an idea of the potential well modification due to the interaction.

In fig. 6, we have $\mathbb{R}_e$P2, 2 versus δ for $\mu\sigma_p = 0,2,5$ and for $\tau = 200$.

We want to point out now (see fig. 6) that the quadrupole mode (2,2) tends to become stable as $\mu\sigma_p$ decreases (for the same potential well modification). For $\mu\sigma p = 0$ the motion (at least in the investigated range) is always stable" This behaviour is in agreement with the properties of the bunch lengthening phenomenon. It is indeed just a single bunch effect. Then it must be generated by low-Q elements (elements whose response falls to zero rapidly ($\mu\sigma p$ large».

As an example, we have plotted, in fig. 7 a,b,c) $\mathbb{R}_e$P2, 2 versus δ and the values of $\bar{\Delta}$ obtained with the simulation (25) after 7 x 10^3 machine turns. We have.

$$\tau = 200, \quad \Omega_o = 10^{-2}$$

and,

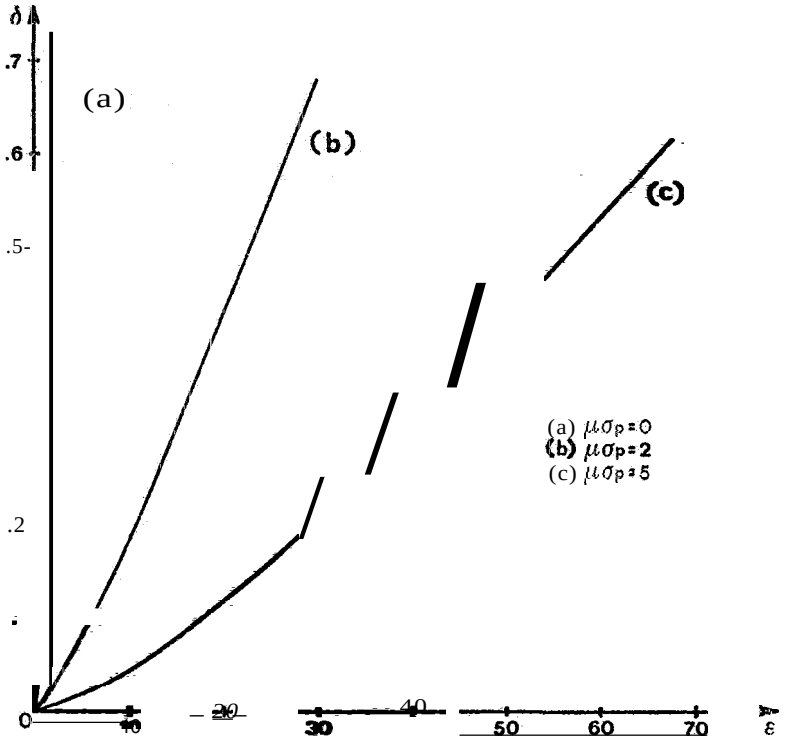
δ
.7
.6
.5-
.2
(a)
(b)
(c)
(a) μσp=0
(b) μσp=2
(c) μσp=5
0
40
30
50
60
70
ε

FIG. 5

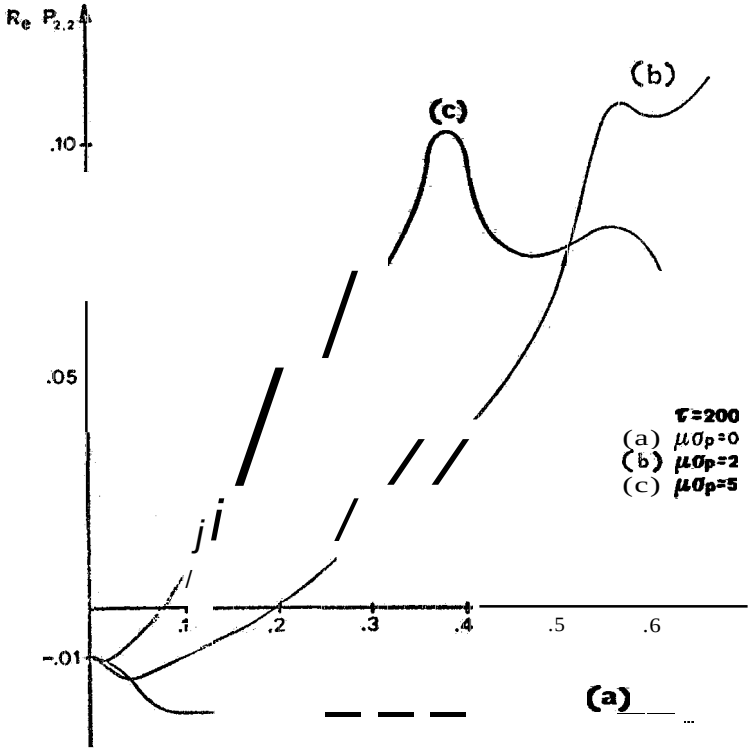
Re P2,2
.10
.05
-.01
(b)
(c)
τ=200
(a) μσp=0
(b) μσp=2
(c) μσp=5
.1
.2
.3
.4
.5
.6
(a)

FIG. 6

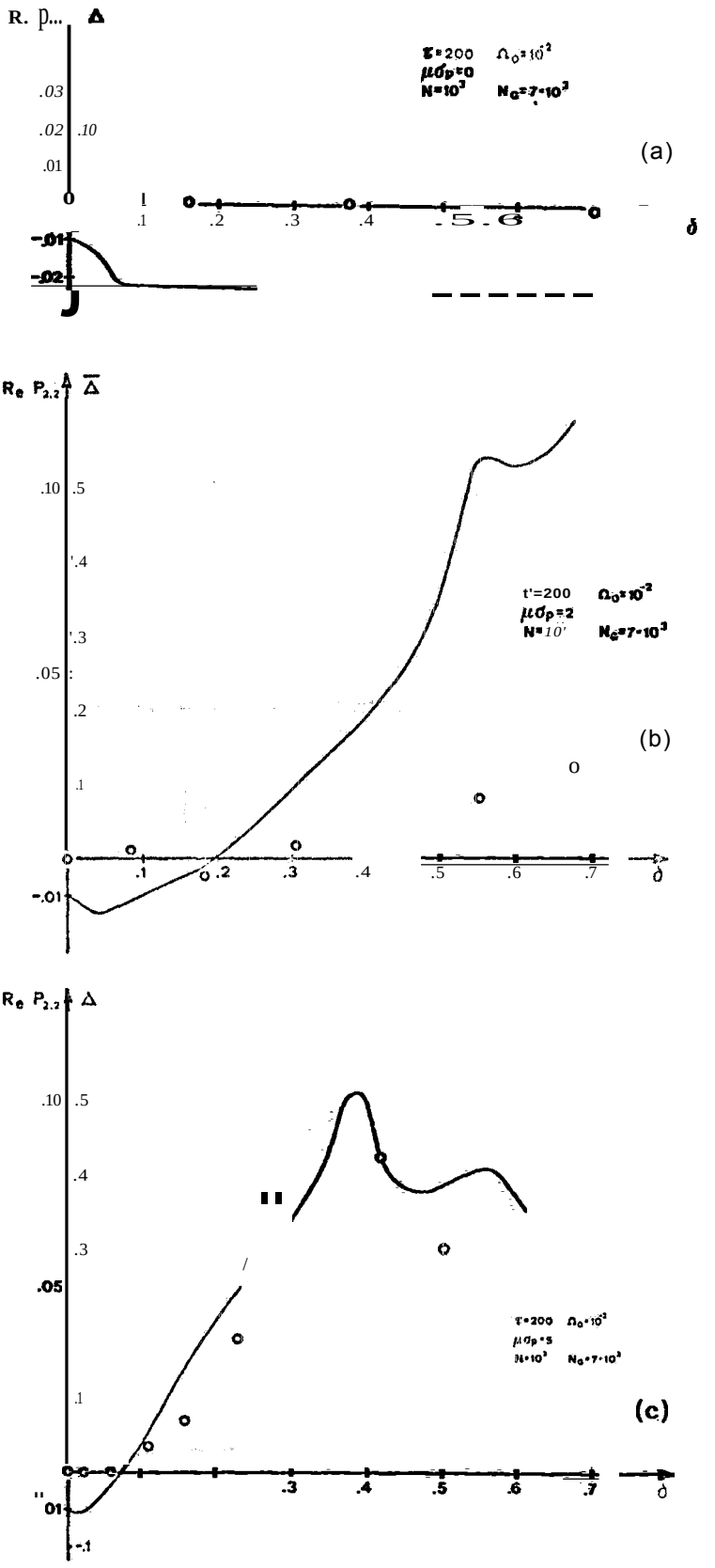
R. p...
.03
.02
.10
.01
0
.1
.2
.3
.4
.5
.6
δ
-.01
-.02
(a)
Re P2,2
.10
.5
.4
.3
.05
.2
.1
-.01
.6
.7
(b)
Re P2,2
.10
.5
.4
.3
.05
.1
.3
.4
.5
.6
.7
-.1
(c)

FIG. 7

FIG,. 713.) $\mu\sigma_p = 0$ stable motion

FIG, 7b) $\mu\sigma_p = 2$ } unstable motion above

FIG, 7c) $\mu\sigma_p = 5$ } the threshold $\mathbb{R}_e P2,2 = 0$.

The other quadrupole mode (2,0) becomes unsta.ble at higher δ values. Therefore this mode does not determine the threshold. The dipole mode (1, 1) becomes unstable at lower values (with respect to the (2, 2) mode); but does not seem to affect the energy spread blow up (as it may be expected).

In fig. 8 the values of $\mathbb{R}_e p_{1,1}$, $\mathbb{R}_e p_{2,0}$ and $\mathbb{R}_e p_{4,0}$ are plotted versus δ for $\tau = 200$ and $\mu\sigma_p = 5$.

It is interesting to note that, at first, mode (2,0) coalesces with mode (4, 0), then they become unstable together.

Let us now consider the case investigated in fig. 2. The agreement between the F. P. solution (23) and the simulation is due to the stability of the time-independent distribution. We have plotted, in fig. 9, $\mathbb{R}e\, P2,2$ for $\tau = 10$ and $\mu\sigma_p = 5$.

We may see that (in the investigated region, $\varepsilon = 30$, that is $\delta = .21$) the motion is stable.

9. - NUMERICAL EXAMPLE

In this section we evaluate the order of magnitude of the impedence Zo (see eq. (4)), that would produce the effect we are talking about. We consider the case of fig. 4, that is,

(59) $$\tau = 200, \qquad \mu\sigma_p = 5$$

In this condition the stability thre.shold is,

(60) $$\varepsilon_{th} \simeq 15$$

From eqs. (13) anel (21), we obtain,

(61) $$\varepsilon = \frac{Z_o \mathbb{e}^2 N \omega_0 \, a}{2\pi E_o \sigma_p}$$

The bunch current I is defined by the equation,

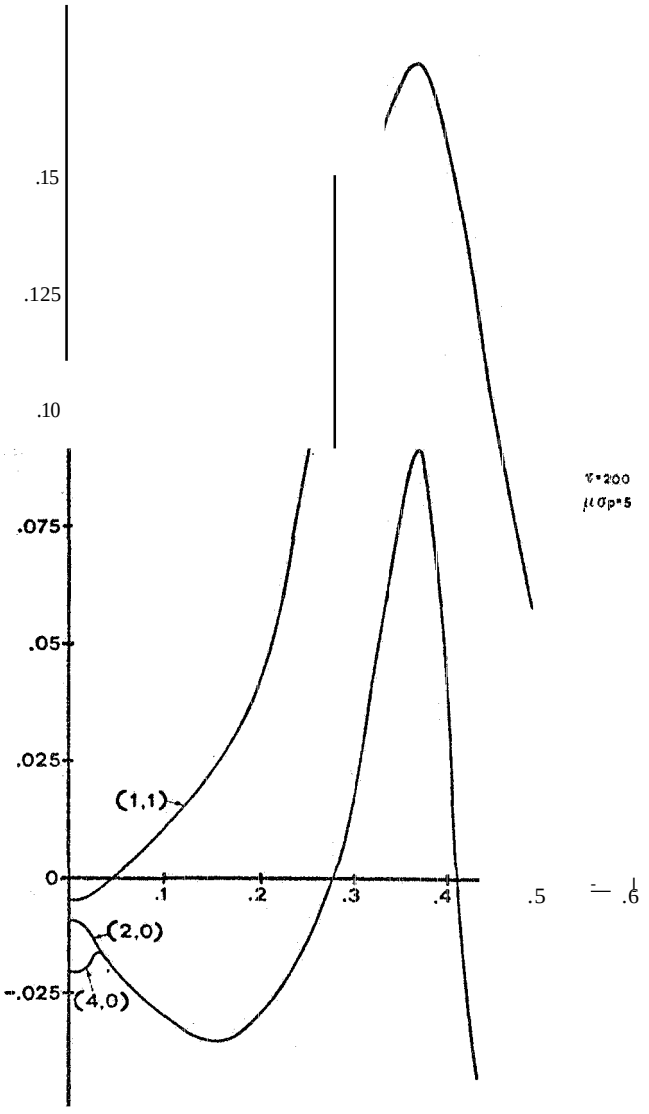

FIG. 8

(62) $$1 = eN\frac{\omega_o}{2\pi}$$

From eqs. (61), (62) and if we measure the working energy Eo in eV, we obtain,

(63) $$\varepsilon \cdot \frac{(12_o)\,\alpha}{E_a \text{ or } \frac{2}{p}} \quad (\mu \sigma_p).$$

We consider the following conditions (tested, for example, in ADONE),

(64) $$E_o = 500 \text{ MeV}, \frac{\sigma_p}{\alpha} = 2 \times 10^{-4}., \quad I = \text{lmA}, \quad = 6.6\text{xl}0\text{-}^2$$

If we insert eqs. (59), (60) and (64) into eq. (63), we obtain,

(65) $$2_o \approx 4\ \text{K}\Omega$$

As an order of magnitude, we may consider the value of 121 given by cross section changes in a vacuum chamber(22),

(66) $$|Z| \approx N_c(\text{lOO(S-I)})\ \Omega$$

where N_c is the number of discontinuities in the vacuum chamber and S is the ratio between the large dimension to the small one. If we put,

$$S = 2,$$

we have (for' 21 $\approx$ 4 KΩ),

$$N_c \approx 40$$

We may actually have such a number of discontinuities (or more) in a storage ring vacuum chamber. However this is only an order of magnitude consideration.

10. - CONCLUDING REMARKS -

The bunch lengthening and the anomalous energy spread may be explained by .aturbolent bea.m model(12, 13).

It is relatively easy to evaluate the threshold for this process ($R_e p_{2,2} = 0$). On the other hand systematic quantitative investigation is very difficult to perform. This is due to the time required for the com

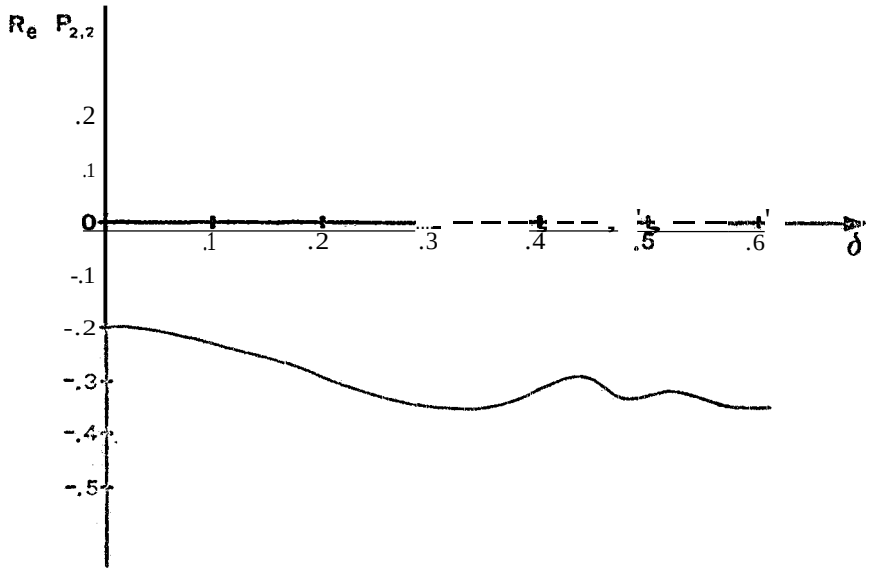

FIG. 9

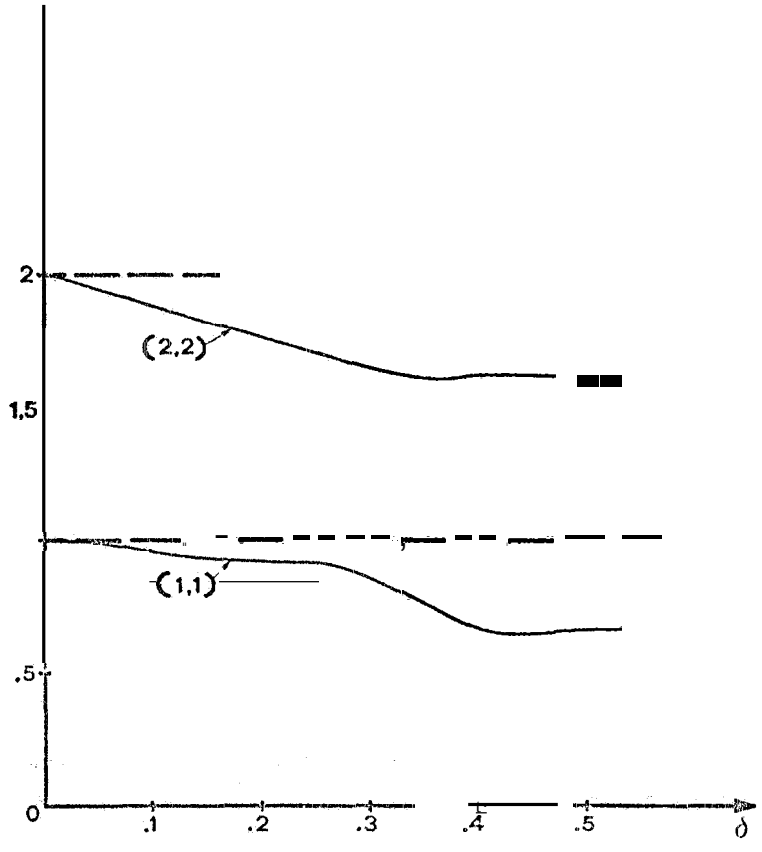

FIG. 10

puter simulation.

It is possible, however, to draw the following conclusions (al though any analytical expression, like eq. **(I),** for the bunch length - has not be,en found)::

a) 'The agreement between the numerical simulation (bunch with a finite number of particles and use of difference equations) and the Fokker-Planck equation(conunuous beam! and differential equation), pro yes that the effect does not depend on the "discrete structure" of the - bunch and that the synchrotron motion is really a "slow motion".

b) All elemEmts that generate fields that are constant over the time of passage of the bu.nch, do not contribute to the anomalous lengthening (see sect. 8). This means that a very strong parameter is the signal variation along the beam (short-r\ange wake fields).

c) The knowledge of the frequenoy shift of the synchrotron motion and its harmonics, may be useful to test the theory and to recognize the elements that may generate the anomalous lengthening. This kind of measure has been performed at SPEAR(23). As an example we have plotted versus δ (see fig. 10) the quantities,

$$|\mathrm{Im}\, p_{1,1}|, \quad |\mathrm{Im}\, p_{2,2}|,$$

in the case,

$$\gamma = 200, \qquad \mu\sigma_p = 5.$$

d) Finally we remark that beam ,energy is a strong parameter. Actually we have that the threshold for the turbulent transition depends on the radiation damping time which, in turn, strongly, depends on the beam energy ($\tau \propto (1/E_o^3)$).

ACKNOWLEDGMENT -

The author is indebted to Prof. M. Bassetti and to Prof. S. Tazzari for many helpful discussions, comments and suggestions.

REFERENCES-

(1) - Group ACO, Allongement de Paquets dans ACO, Orsay Report R. T. 34-69 (1969).
(2) - ADONE Group, Status report on the electron-positron storage Ring, Adone, Proc. of the Particle Accelerator Conf., Chicago, (1971).
(3) - B. Richter, Operating results from SPEAR, Proc. of the Particle Accelerator Conf., San Francisco (1973).
(4) - See, for example, M. Sands, The physics of electron-positron storage rings, an introduction, Heport SLAC··121 (1970).
(5) - J. R. Le Duff, PEP Note nO 71 (1973 PEP Summer Study), Stanford, Berkeley.
(6) - SPEAR Group, SPEAR II performance - Proe:. of thePartic1e Accelerator Conf., Washington (1975).
(7) - J. R. Le Duff, M. P. Level and H. Petit, Orsay Report NI/31-73 (1973).
(8) - Gruppo ADONE, ADONE Internal Report RM-·?, (1975) (in italian).
(9) - K. W. Robinson, LEAL-TM 183 (1969).
(10) - C. Pellegrini and A..M. Sessler, Nuovo Cimento 3A, 116 (1971).
(11) - G.H. Rees, PEP Note N. 43 (1973 PEP Summer Study), Stanford, Berkeley.
(12) - A.N. Lebedev, Frascati Report, LNF-69/52 (1969).
(13) - A. M. Sessler, PEP Note nO 28, LBL Berkeley (1973).
(14) - E. Ferlenghi, Nuovo Cimento 48 B, 73 (1967).
(15) - C. Pellegrini and A.M. Sessler, Nuovo Cimento, 53 13, 198 (1968).
(16) - H. G. Hereward, PEP Note nO 53 (1973 PEP Summer Study), Stanford, Berkeley.
(17) - E.M. Row'e and W. S. Tr'zeciak .. Proc. of the IX Internat. Conf. on High Energy Accelerators, Stanford (1974).
(18) - H. Bruck, Accélérateurs circulaires de particules (Presses Universitaires de France, 1966), pag. 265.
(19) - C. Pellegrini and A. Renieri, ADONE-Internal report T-64 (1974).
(20) - M. Bassetti, Frascati Report LNF..67/45 (1967).
(21) - See, for example, M. Abramowitz and 1. A. Stegun, Handbook of Mathematical Functions, (Dover Jl970), pag. 771.
(22) - H.G. Hereward, CERN/ISR-DI/'75-47 (1975).
(23) - M.A. Allen, G.E. Fischer et al., Some observations on bunch lengthening at SPEAR, Proc. of the IX Int.Conf. on High EneI' gy Accelerators, Stanford (1974).
(24) - F. Amman, Electron and positron storage rings. Present s:Ltuation and future prospects, Proc. of the VIII Intern. Conf. on High Energy Accelerators, CERN (1971).

(25) - M. P. Level and H. Petit, Orsay Report, RT/3.-75 (1975).
(26) - During the printing of this paper, we have received the work of JP. 1. Channel, where the turbulence effect in bunched beams is i.nvestigated: P. 1. Channel, Strong turbulence and the anomalous length of stored particle beams - (Ph. D. Thesis) - LBL-4433 (Berkeley, November 1975).